Real-time Phase Recovery of Biological Cell in Digital Holographic Microscopy by Use of a Self-Calibration Hologram

Tristan Colomb, Jonas Kühn, Florian Charrière and Christian Depeursinge

Ecole polytechnique fédérale de Lausanne,
Institute of imaging and applied optics,
CH-1015 Lausanne, Switzerland
tristan.colomb@a3.epfl.ch

Pierre Marquet

Centre de Neurosciences Psychiatriques, Département de psychiatrie DP-CHUV, Site de Cery,
1008 Prilly-Lausanne, Switzerland

Nicolas Aspert

Lyncée Tec SA,
PSE-A,
CH-1015 Lausanne, Switzerland

Abstract: We demonstrate in Digital Holographic Microscopy a self-calibration hologram method allowing aberrations compensation and a real-time biological cell phase recovery by using a single hologram without adjustment of any parameters.

OCIS codes: (090.1760) Computer holography; (090.1000) Aberration compensation; (180.3170) Interference microscopy

1. Introduction

Digital Holographic Microscopy (DHM) is a powerful instrument for real-time phase-contrast imaging since the reconstruction of this phase-contrast can be achieved from a single hologram with the help of parameters adjusted by fitting procedures [1] or substraction of a reference phase in the reconstruction plane [2]. Furthermore, the digital approach allows parasitic interferences suppression [3], compensation for spherical aberration [4], astigmatism [5] among others. These numerical procedures allow to recover quantitative visualization of living cells with subwavelength axial accuracy [6], but need most of the time parameters adjustment [1] or a reference hologram acquisition [2].

In this paper, we present a simple method called Self-Reference Conjugated Hologram (Self-RCH), inspired by the works of Upatnieks *et al.* [7] and Ward *et al.* [8], that allows a calibration of the DHM setup by compensating for the phase aberrations and image distortion without iterative procedures or parameters adjustment. We show that the Self-RCH method allows to reconstruct a non-aberrated wavefront in term of amplitude and phase from this hologram. We demonstrate the method by a real-time phase reconstruction of the motion of Trypanosoma Brucei.

2. Principle

Figure 1 presents typical DHM setups in transmission configurations. The architecture is based on a modified Mach-Zehnder interferometer. A MO, collecting the wave transmitted through or reflected by the specimen, produces an object wave $\boldsymbol{O}$ forming a magnified image of the specimen behind the CCD camera at a distance $d \cong 5$ cm. A lens or a similar MO [9] could be introduced in the reference arm (RL) to produce a spherical reference wave $\boldsymbol{R}$ in the CCD with a curvature plane very similar to the curvature induced by the MO.

The interference between the reference and object waves produces at the exit of the interferometer the hologram digitalized by the CCD camera:

$$I_H(k,l) \quad = (\boldsymbol{R}+\boldsymbol{O})(\boldsymbol{R}+\boldsymbol{O})^* = |\boldsymbol{R}|^2 + |\boldsymbol{O}|^2 + \boldsymbol{R}^*\boldsymbol{O} + \boldsymbol{R}\boldsymbol{O}^*, \tag{1}$$

where k,l are integers. The two first terms form the zero-order term, the third and fourth terms are respectively the

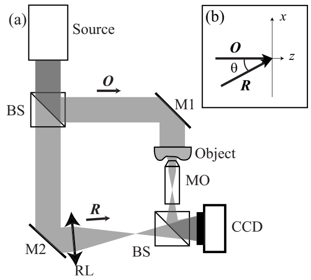

Fig. 1: Transmission digital holographic microscope. ***O*** object wave; ***R*** reference wave; BS beam splitter; M1, M2 mirrors; MO microscope objective, RL lens in the reference wave, OC condenser in the object wave. (b) Detail of the off-axis geometry.

virtual and real image terms. Example of hologram and its respective spectrum (the zero-order term is already filtered) are presented in Fig. 2.

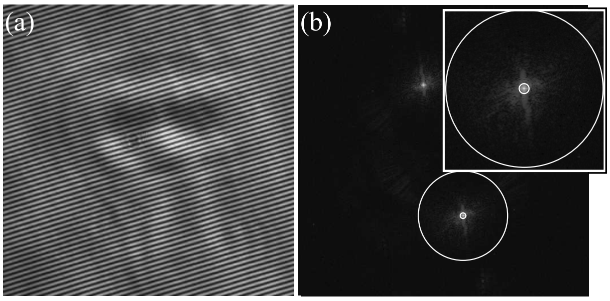

Fig. 2: (a) 256x256 pixels area of a 512x512 hologram of Trypanosoma Brucei; (b) spectrum and detail of virtual image frequencies on the upper right; the big circle (radius 80 pixels) delimits the frequency for the sample hologram and the small one (radius 10 pixels) the filtering for Self-RCH.

Usually, the reference wave ***R*** and object wave ***O*** are assumed to be plane or spherical waves. We assume here that the reference wave is non-aberrated as in Refs. [7, 8] and define more generally the object wave by introducing a phase aberration term $W_{\boldsymbol{O}}$ to a plane object wave (the same reasoning can be done with a spherical wave). Finally, we assume that the specimen does not introduce further phase aberrations but only a phase delay $\varphi(x, y)$ coming from a refractive index or/and thickness difference. The waves can also be written as:

$$\boldsymbol{R}(x,y) = |\boldsymbol{R}| \cdot \exp\left[i(k_x x + k_y y)\right], \quad (2)$$
$$\boldsymbol{O}(x,y) = |\boldsymbol{O}(x,y)| \exp\left[i\varphi(x,y)\right] \cdot \exp\left[iW_{\boldsymbol{O}}(x,y)\right], \quad (3)$$

where k_x, k_y define the direction propagation associated to the angle θ defined in Fig. 1(b).

The reconstructed wavefront Ψ of the virtual image is computed by multiplying the filtered digital hologram I_H^F [Fig. 2(b) with large circle] [3]

$$I_H^F = \boldsymbol{R}^*\boldsymbol{O} = |\boldsymbol{R}||\boldsymbol{O}| \exp\left[-i(k_x x + k_y y)\right] \exp\left[i(\varphi + W_{\boldsymbol{O}})\right], \quad (4)$$

by a digital reference wave $\boldsymbol{R}_D = \exp\left[i(k_x k\Delta x + k_y l\Delta y)\right]$ and by computing numerically the wave front at a distance *d*. Let us replace $\boldsymbol{R}_D$ by a more general complex numbers array Γ_{RCH}^H. The reconstructed wavefront expressed in convolution formulation is therefore

$$\Psi(m,n) = A \cdot \mathrm{DFT}^{-1}\left\{\mathrm{DFT}\left[\Gamma_{RCH}^H(k,l) I_H^F(k,l)\right] \cdot \exp\left[-i\pi\lambda d(\nu_k^2 + \nu_l^2)\right]\right\}. \quad (5)$$

where, DFT is the Discrete Fourier Transform; *m*, *n*, *k*, *l* are integers ($-N/2 < m, n, k, l \leq N/2$); *d*, the reconstruction distance; $A = \exp(i2\pi d/\lambda)/(i\lambda d)$; λ, the wavelength; $\nu_k = k/(N\Delta x)$, $\nu_l = l/(N\Delta y)$ are the coordinates in the spatial frequencies.

Equations 4 and 5 show that the term $W_{\boldsymbol{O}}$ is propagated in the reconstruction plane. The goal of our method is to compensate for the aberrations in the hologram plane with the introduced Γ_{RCH}^H array defined as a Self-Reference

Conjugated Hologram as follows. Let us assume that the object is quite smooth as a biological cell. Because the information of the details of the sample have higher frequencies than the aberrations (contained in the central frequency), we compute the self-reference hologram $I_H^{R,F}$ by filtering strongly the spectrum to keep only the central frequency of the virtual image [small circle of 10 pixels radius in Fig. 2(b)]. This self-reference hologram is also written:

$$I_H^{R,F} = \boldsymbol{R}^*\boldsymbol{O} = |\boldsymbol{R}||\boldsymbol{O}| \exp\left[-i(k_x x + k_y y)\right] \exp\left[iW_{\boldsymbol{O}}\right]. \tag{6}$$

Γ_{RCH}^H is defined as the conjugated phase of Eq. 6:

$$\Gamma_{RCH}^H(m,n) = \arg\left[I_H^{R,F*}\right] = \exp\left[i(k_x x + k_y y)\right] \exp\left[-iW_{\boldsymbol{O}}\right]. \tag{7}$$

The multiplication of Γ_{RCH}^H with the specimen hologram (Eq. 4) gives:

$$\Gamma_{RCH}^H(m,n) \cdot I_H^F = |\boldsymbol{R}||\boldsymbol{O}| \exp\left[i\varphi(x,y)\right]. \tag{8}$$

Equation 5 is therefore a propagation of a plane wave without aberrations terms.

Figure 3 presents frames of a movie of 3D plot of phase images, reconstructed from a sequence of holograms recorded at 20 frames per second. The noise level around the specimen is evaluated by computing a standard deviation of 2.7 degrees, the phase delay introduced by the specimen have a maximum of 25 degrees. We see clearly the movement of the two cells.

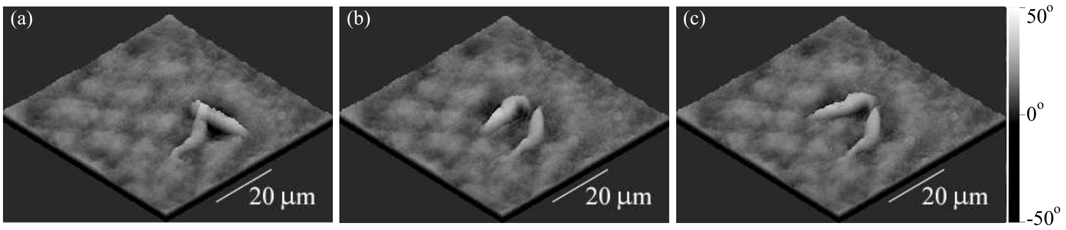

Fig. 3: Phase reconstruction of Trypanosoma Brucei by Self-RCH method during time; (a) t=0 ms (b) t=50 ms and (c)100 ms

3. Conclusion

We present in this paper a simple calibration method called Self-Reference Conjugated Hologram that allows from a single hologram acquisition the phase recovery of biological cell without parameters adjustment. A noise level less than 3 degrees was demonstrated for the phase reconstruction sequence. Furthermore this technique compensate for the aberrations and would allow to reduce the the cost of the setup by using low cost optics presenting aberrations.

References

1. T. Colomb, E. Cuche, F. Charrière, J. Kühn, N. Aspert, F. Montfort, P. Marquet, and C. Depeursinge., “Automatic procedure for aberrations compensation in digital holographic microscopy and applications to specimen shape compensation,” Appl. Opt. (in press).
2. P. Ferraro, S. D. Nicola, A. Finizio, G. Pierattini, and G. Coppola, “Recovering image resolution in reconstructing digital off-axis holograms by Fresnel-transform method,” Appl. Phys. Lett. **85**, 2709–2711 (2004).
3. E. Cuche, P. Marquet, and C. Depeursinge, “Spatial filtering for zero-order and twin-image elimination in digital off-axis holography,” Appl. Opt. **39**, 4070–4075 (2000).
4. S. de Nicola, A. Finizio, G. Pierattini, D. Alfieri, S. Grilli, L. Sansone, and P. Ferraro, “Recovering correct phase information in multiwavelength digital holographic microscopy by compensation for chromatic aberrations,” Opt. Lett. **30**, 2706–2708 (2005).
5. S. Grilli, P. Ferraro, S. D. Nicola, A. Finizio, G. Pierattini, and R. Meucci, “Whole optical wavefields reconstruction by digital holography,” Opt. Express **9**, 294–302 (2001).
6. P. Marquet, B. Rappaz, P. J. Magistretti, E. Cuche, Y. Emery, T. Colomb, and C. Depeursinge, “Digital holographic microscopy: a noninvasive contrast imaging technique allowing quantitative visualization of living cells with subwavelength axial accuracy,” Opt. Lett. **30**, 468–470 (2005).
7. J. Upatnieks, A. V. Lugt, and E. Leith, “Correction of lens aberrations by means of holograms,” Appl. Opt. **5**, 589–593 (1966).
8. J. Ward, D. Auth, and F. P. Carlson, “Lens Aberration Correction by Holography,” Appl. Opt. pp. 896–900 (1971).
9. C. J. Mann, L. Yu, C.-M. Lo, and M. K. Kim, “High-resolution quantitative phase-contrast microscopy by digital holography,” Opt. Express **13**, 8693 – 8698 (2005).